Mechanism and Machine Theory 108 (2017) 191–208

Contents lists available at ScienceDirect

Mechanism and Machine Theory

journal homepage: www.elsevier.com/locate/mechmachtheory

Modeling and dynamic behavior analysis of a coupled multi-cable double drum winding hoister with flexible guides

Ji Wang[a,b], Yangjun Pi[a,b,*], Yumei Hu[a,b], Xiansheng Gong[c]

[a] State Key Laboratory of Mechanical Transmission, Chongqing University, Chongqing 400044, China
[b] College of Automotive Engineering, Chongqing University, Chongqing 400044, China
[c] College of Mechanical Engineering, Chongqing University, Chongqing 400044, China

ARTICLE INFO

Keywords:
Nonlinear vibration
Dynamic tension
Flexible guides
Moving string
Winding hoister

ABSTRACT

In this paper, a comprehensive model is derived to analyze the dynamic behavior of a multi-cable double drum winding mining hoister with flexible guides by using Hamilton principle. Each cable which consists of an inclined section and a varying length vertical section is modeled as an axially moving string with coupled transverse-longitudinal nonlinear vibration. The coupling between different cables is described through the dynamic and kinematic equations of the conveyance. The time-varying equal moment of inertia of drums is obtained by considering the varying mass of cables winding on drums. The model of flexible guides which was always approximated as a spring-damping system is modeled as a tensioned string with fixed ends in this paper. The dynamic characteristics of flexible guides are considered in the interaction between the conveyance and the flexible guides via calculating the lateral displacement of the conveyance corner and reaction forces from flexible guides. The dynamic behavior of the multi-cable double drum winding hoister with unbalance factors, the conveyance eccentricity and the drum radius inconformity, are analyzed by simulation. Some design principles are proposed to restrict the inconformity of dynamic tension between cables.

1. Introduction

With the increasing focus on exploitation of deep mineral resources, stable design and operation reliability of hoisters for long distance transport have received increasing attention. The hoisters are used to transport mineral resources in deep mines to the surface platform. To improve the efficiency, the hoisters for long distance transport would work in high-speed and heavy-load conditions [1]. Common single cable winding hoisters are not suitable in the long distance transport with heavy-load, as it needs very burly cable to meet the required strength, which would result in inconvenient cable winding. To solve this problem, the multi-cable winding hoister is introduced, as shown in Fig. 1. It consists of two cables driven by two mechanically jointed drums. The multi-cable wingding hoister is a strong coupled, time varying, nonlinear distributed-parameter system. Compared with single cable winding systems, the multi-cable winding hoisters have more powerful carrying capacity in the long distance and heave-load situation. However, the fast transit and unbalance factors may lead to the excessive vibration and inconformity of dynamic tension between coupled cables. It would result in premature fatigue fracture of cables, which would impact the reliability of operation and require inspections or costly repairs. Therefore, it is necessary to grasp dynamic characteristics of the multi-cable winding hoister and find some design principle to control the inconformity of dynamic tension between cables in the rational range.

* Corresponding author at: State Key Laboratory of Mechanical Transmission, Chongqing University, Chongqing 400044, China.
E-mail address: cqpp@cqu.edu.cn (Y. Pi).

http://dx.doi.org/10.1016/j.mechmachtheory.2016.10.021
Received 22 November 2015; Received in revised form 8 October 2016; Accepted 25 October 2016
Available online 14 November 2016
0094-114X/

Nomenclature

$u_{vi}(x, t)$	Longitudinal elastic displacement of the ith vertical rope.
$w_{vi}(x, t)$	Transverse elastic displacement of the ith vertical rope.
$u_{ci}(x, t)$	Longitudinal elastic displacement of the ith catenary rope.
$w_{ci}(x, t)$	Transverse elastic displacement of the ith catenary rope.
R_d	Radius of the drums.
R_s	Radius of the head sheaves.
J_d	Inertia moment of the drum.
J_c	Inertia moment of the conveyance.
$\tilde{J}_d(t)$	Time-varying equal inertia moment of the drums.
$V(t)$	Target hoisting velocity.
$a(t)$	Target hoisting acceleration.
$V_C(t)$	Longitudinal velocity of the conveyance centroid.
$W_C(t)$	Transverse velocity of the conveyance centroid.
$\varphi(t)$	Angle of the conveyance.
A	Cross-sectional area.
E	Young's modulus.
$\overline{T}_{ci}(x, t)$	Static tension in the catenary section of the ith cable.
$\overline{T}_{vi}(x, t)$	Static tension in the vertical section of the ith cable.
$T_{ci}(x, t)$	Dynamic tension in the catenary section of the ith cable.
$T_{vi}(x, t)$	Dynamic tension in the vertical section of the ith cable.
T_0	Gravity force of the conveyance.
L_0	Initial length of the vertical cable.
$a_{VC}(t)$	Longitudinal acceleration of the conveyance centroid.
$a_{WC}(t)$	Transverse acceleration of the conveyance centroid.
$L_{vi}(t)$	Time-varying length of the vertical section in the ith cable.
L_{ci}	Length of the catenary section in the ith cable.
L_g	Length of the flexible guides.
$M_i(t)$	Equal load of the ith cable.
e	Eccentricity from the mass center of the conveyance.
S_i	Distance between the ith cable and the conveyance centroid.
$f_{cl}(t)$	Counterforce from the left flexible guide.
$f_{cr}(t)$	Counterforce from the right flexible guide.
c_{tc}	Transverse damping coefficient of the catenary rope.
c_{lc}	Longitudinal damping coefficient of the catenary rope.
c_{tv}	Transverse damping coefficient of the vertical rope.
c_{lv}	Longitudinal damping coefficient of the vertical rope.
c_s	Damping coefficient between the cable and the head sheave.
d_s	Length of the sticking zone at the head sheave.
θ	Angle between the catenary rope and horizontal plane.
T_g	Pretension of the flexible guide.
E_g	Young's modulus of the flexible guide.
A_g	Cross-sectional area of the flexible guide.
$c(t)$	Position of the conveyance centroid on the flexible guide.
$w_{gl}(c(t), t)$	Transverse elastic displacement of the left flexible guide at $c(t)$.
$w_{gr}(c(t), t)$	Transverse elastic displacement of the right flexible guide at $c(t)$.

There are not many researches focusing on dynamic modeling of mining winding hoisters. Mathematically, the dynamic model of the hoister is similar with winding elevators. A transverse vibration model of an elevator with arbitrarily varying length was proposed in [2,3]. He et al. [4] built a varying length, varying speed elevator model with transverse vibration. Sandilo and van Horssen [5,6] built a dynamic model to describe the lateral vibrations of an elevator. By Wu and Zhu [7] and Zhang et al. [8], a single cable elevator considering coupled transverse and longitudinal vibrations was introduced for the study of vibration energy. Kumaniecka and Niziol [9] studied the longitudinal-transverse vibration of a hoister and analyzed parametric resonances of the rope. Most of current researches on dynamic modeling of hoisters or elevators are limited in the single cable winding type, which can not represent the coupled dynamic behavior between the different cables of the multi-cable winding hoister.

The literatures on the dynamic modeling of the multi-cable double drum winding hoisters are scarce. Recently, a model of double drum winding mine hoister was proposed by Kaczmarczyk and Ostachowicz [10], and the effect of hoisting velocity on the vibration response of hoist cables was investigated by simulation [11]. In his research, an equivalent catenary and an equivalent vertical rope, supporting one-half of the full weight of the conveyance, represented the two actual catenaries and two vertical ropes with a movable pulley. The coupling between different cables in the multi-cable double drum winding hoister was not investigated. It is an important factor on the station and safety of the multi-cable winding mine hoisters used for the high-speed,heavy-load and long distance transport.

In addition, dynamic interactions between the conveyance and the flexible guides plays an important role in deep mine exploitation. Counterforce of flexible guides would affect the stability of the conveyance moving at high speed considerably. The elastic support of flexible guides was always approximate as a spring-damping system in the previous researches. Garkusha and Dvornikov [12] investigated a rod-shaped elevator supported by elastic guides with constant support rigidity. Terumichi et al. [13], Zhu and Xu [14] proposed a time-varying length string with a mass supported by a viscoelastic guide with constant stiffness and damping coefficient. Ghayesh et al. [15,16] also studied an axially moving string supported by a partial viscoelastic guide analytically. Chirkov [17] and Wang et al. [18] represented analytically the dependence between the position of the contact point and the transverse rigidity of the elastic guide. However, the dynamic characteristics of flexible guides are not included in the description of

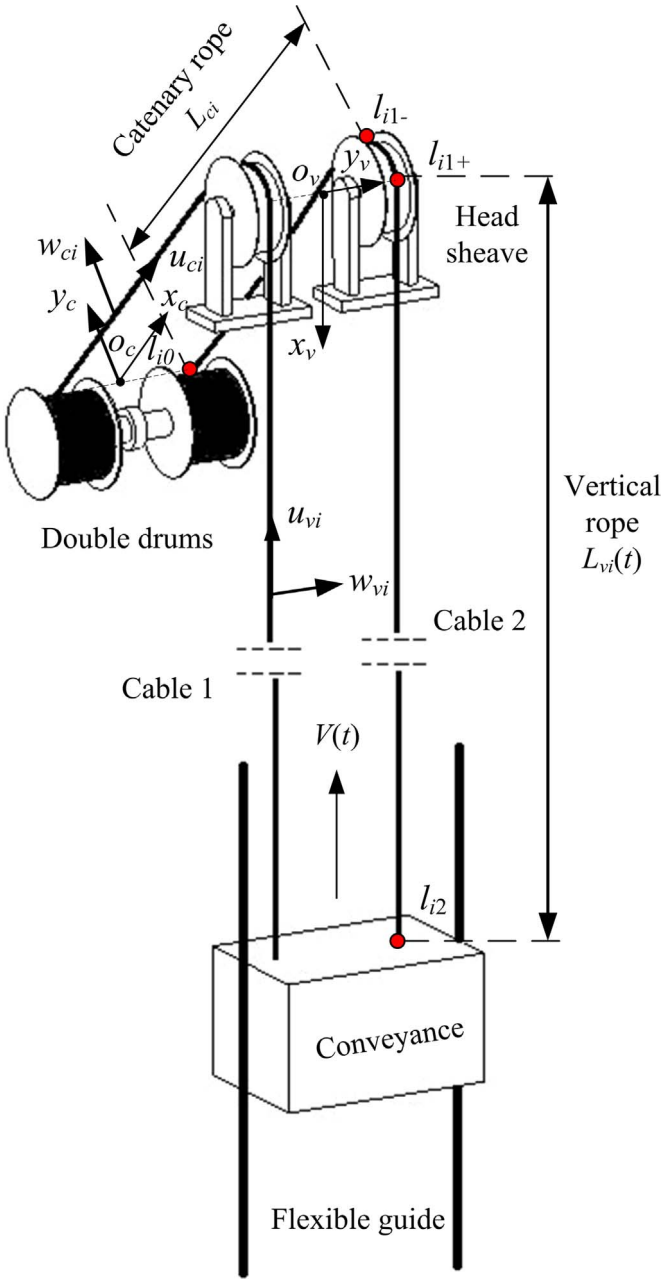

Fig. 1. Diagram of a multi-cable winding hoister with double drums.

the interaction behavior between flexible guides and the conveyance, which cannot accurately represent the dynamic interaction between flexible guides and the conveyance, especially in the situation of the high-speed hoisting.

In this paper, the dynamic model of a multi-cable double drum winding hoister with flexible guides is derived via Hamilton principle, considering the coupling between different cables through the dynamic and kinematic equations of the conveyance. Each cable is built as a transverse-longitudinal vibration axially moving string which consists of an inclined section and a time-varying length vertical section. The two sections are coupled at head sheave and the friction between cables and head sheave are considered as well. Considering the mass of cables winding on drums would vary in a wide range for the long-distance hoister, the equal time-varying inertia moment of the drums is obtained. In addition, the model of flexible guides is built as a tensioned string and the dynamic characteristics of flexible guides are considered in the interaction between the flexible guides and the conveyance. In this hoister system, four groups of nonlinear partial differential equations (PDEs) govern the coupled longitudinal and transverse vibration of two cables with two sections. The infinite dimensional distributed-parameter system is discretized by the Finite Difference Method. The effects of the conveyance eccentricity and the radius inconformity between drums on the dynamic behavior

of a multi-cable double drum winding mining hoister with flexible guides are investigated under the high-speed, heavy-load conditions. Several design principles have been proposed to restrict the inconformity of dynamic tension between different cables.

Comprehensive modeling and dynamic behavior analysis of the multi-cable double drum winding hoister system are significant to the exploitation of deep mineral resources. To our knowledge, the researches on comprehensive modeling of the multi-cable double drum winding hoisters, including the coupling between cables, time-varying inertia moment of drums and dynamic characteristics of the flexible guides have not been performed. The main contributions of this article are summarized as follows:

1) The dynamic model of the multi-cable winding mining hoister with double drums is built. Coupling between different cables is described through the dynamic and kinematic equations of the conveyance. The time-varying equal inertia moment of drums is included in this model via considering the varying mass of cables winding on the drums.
2) The flexible guide which was always approximate as a spring-damping system is modeled as a tensioned string with fixed ends in this paper. Dynamic characteristics of flexible guides are considered in the mathematical description of the interaction behavior between the conveyance and the flexible guides.
3) Some design principles to restrict the inconformity of dynamic tension between different cables of the multi-cable double drum winding mining hoister are proposed.

The rest of this paper is organized as follows. In Section 2, the dynamic model of the multi-cable winding hoister with double drums is derived. In section3, the equations of model are discretized by the Finite Difference Method. In section4, the numerical simulation and discussion are carried out to show the dynamic behavior of the hoister. Finally, the conclusion of this paper is presented in Section 5.

2. Modeling of the multi-cable winding hoister

A typical multi-cable winding hoister with double drums is showed in Fig. 1. It includes two mechanically jointed winding drums, winded by two cables passing over two head sheaves.

Cables connect with a conveyance which contacts with two tensioned flexible guides, showed in Fig. 2,

where r_d is the distance from the mass center of the conveyance to the connect point between the conveyance and cables. r_z is the distance from the mass center to the corner of the conveyance. l_d is the distance between two connect point on the conveyance. l_t is the distance between two head sheaves. l_l is the distance between cables and guides. l_g is the height of the conveyance. l_z is the length of the conveyance. β is half of the angle between two connect point and the mass center of the conveyance. ϕ is the angle between the corner, the mass center and the midpoint of height of the conveyance.

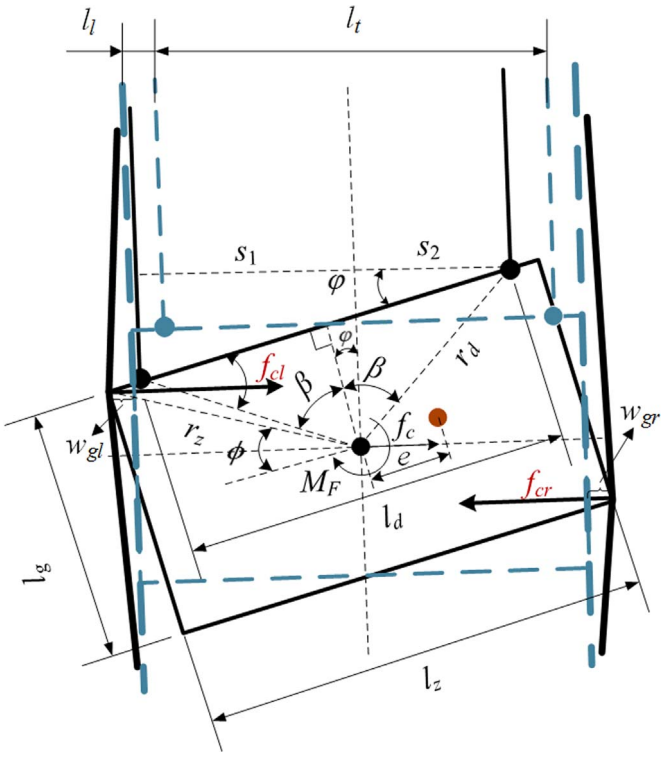

Fig. 2. The interaction between the conveyance and the flexible guides.

The dynamic responses of hoisting cables are usually classified as lateral and longitudinal vibrations in the catenary and the vertical ropes [19]. In this paper, each hoisting cable consists of the catenary and vertical ropes. They are built as coupled transverse-longitudinal vibration axially moving strings with constant length and varying length respectively. Two fixed frames of reference, $o_c x_c y_c$ and $o_v x_v y_v$, are established in the middle of the two cables, corresponding to the contact points of the drum and the head shave respectively. l_{i0}, l_{i1-}, l_{i1+}, l_{i2} are defined as the tangent point of the driving drum, two tangent points of the head sheave, and the junction point on the conveyance respectively for ith cable, showed in Fig. 1. For clarity, notations $()' = \partial()/\partial x$, $\dot{()} = \partial()/\partial t$ are used throughout this paper. The total kinetic energy of the multi-cable winding hoister with two drums can be represented as

$$\begin{aligned} E_k = {} & \tfrac{1}{2}\rho \textstyle\sum_{i=1}^{2} \int_{l_{i0}}^{l_{i1-}} [(V(t)w'_{ci}(x_c,t) + \dot{w}_{ci}(x_c,t))^2 + (V(t)u'_{ci}(x_c,t) + \dot{u}_{ci}(x_c,t) + V(t))^2]dx_c \\ & + \textstyle\sum_{i=1}^{2} \tfrac{1}{2}\left(\frac{V(t)+\dot{u}_{ci}(l_0,t)}{R_d}\right)^2 J_d + \tfrac{1}{2}(L_{vi}(0) - L_{vi}(t))\rho(V(t) + \dot{u}_{ci}(l_0,t))^2 \\ & + \textstyle\sum_{i=1}^{2} \tfrac{1}{2}\left(\frac{V(t)+\dot{u}_{ci}(l_{1-},t)}{R_s}\right)^2 J_s + \tfrac{1}{2}\rho \textstyle\sum_{i=1}^{2} \int_{l_{i1+}}^{l_{i2}} [(V(t)w'_{vi}(x_v,t) + \dot{w}_{vi}(x_v,t))^2 \\ & + (V(t)u'_{vi}(x_v,t) + \dot{u}_{vi}(x_v,t) + V(t))^2]dx_v + \tfrac{1}{2}MV_C^2(t) + \tfrac{1}{2}MW_C^2(t) + \tfrac{1}{2}J_c\dot{\varphi}^2(t)\,, \end{aligned} \tag{1}$$

where $u_{vi}(x_v, t)$ and $w_{vi}(x_v, t)$ represent the longitudinal elastic displacement and the transverse elastic displacement of the vertical ropes. $u_{ci}(x_c, t)$ and $w_{ci}(x_c, t)$ represent the longitudinal and transverse elastic displacements of the catenary ropes. Where the subscript c, v and i represent the catenary section and vertical section in the ith cable. The potential energy of the multi-cable winding hoister with two drums can be represented as

$$\begin{aligned} E_p = {} & \tfrac{1}{2}\textstyle\sum_{i=1}^{2} EA \int_{l_{i0}}^{l_{i1-}} (u'_{ci}(x_c,t) + \tfrac{1}{2}w'_{ci}(x_c,t)^2)^2 dx_c \\ & + \textstyle\sum_{i=1}^{2} \int_{l_{i0}}^{l_{i1-}} \overline{T}_{ci}(x_c,t)[u'_{ci}(x_c,t) + \tfrac{1}{2}w'_{ci}(x_c,t)^2]dx_c \\ & + \tfrac{1}{2}\textstyle\sum_{i=1}^{2} EA \int_{l_{i1+}}^{l_{i2}} (u'_{vi}(x_v,t) + \tfrac{1}{2}w'_{vi}(x_v,t)^2)^2 dx_v \\ & + \textstyle\sum_{i=1}^{2} \int_{l_{i1+}}^{l_{i2}} \overline{T}_{vi}(x_v,t)[u'_{vi}(x_v,t) + \tfrac{1}{2}w'_{vi}(x_v,t)^2]dx_v\,, \end{aligned} \tag{2}$$

where $\overline{T}_{ci}(x_c, t)$, $\overline{T}_{vi}(x_v, t)$ are the static tension in the inclined catenary section and the vertical section of the ith cable.

The relationship of the conveyance position (x, y) and the positions (x_1, y_1), (x_2, y_2) of ends of cables in the fixed coordinate system $o_v x_v y_v z_v$ can be written as

$$x_1 = x - r_d\cos(\tfrac{\pi}{2} - (\beta + \varphi(t))), \qquad y_1 = y - r_d\sin(\tfrac{\pi}{2} - (\beta + \varphi(t))),$$
$$x_2 = x + r_d\cos(\tfrac{\pi}{2} - (\beta - \varphi(t))), \qquad y_2 = y - r_d\sin(\tfrac{\pi}{2} - (\beta - \varphi(t))). \tag{3–6}$$

The position and velocities of the mass center of the conveyance can be expressed as

$$x = \frac{1}{2}(x_1 + x_2) + r_d\cos\beta\sin(\varphi(t)), \tag{7}$$

$$y = \frac{1}{2}(y_1 + y_2) + r_d\cos\beta\cos(\varphi(t)), \tag{8}$$

$$\begin{aligned} V_C(t) = {} & \tfrac{1}{2}(\dot{u}_{v1}(l_{12},t) + V(t) + \dot{u}_{v2}(l_{22},t) + V(t)) \\ & - r_d cos\beta\sin(\varphi(t))\dot{\varphi}(t), \end{aligned} \tag{9}$$

$$W_C(t) = \frac{1}{2}(\dot{w}_{v1}(l_{12},t) + \dot{w}_{v2}(l_{22},t)) + r_d\cos\beta\cos(\varphi(t))\dot{\varphi}(t). \tag{10}$$

The longitudinal velocities of ends of cables are approximated as the sum of hoisting and vibration velocities $\dot{u}_{vi}(l_{i2}, t) + V(t)$ in Eq. (9). The corresponding acceleration can be obtained as

$$\begin{aligned} a_{VC}(t) = \dot{V}_C(t) = {} & \tfrac{1}{2}(\ddot{u}_{v1}(l_{12},t) + \ddot{u}_{v2}(l_{22},t)) + \dot{V}(t) \\ & - r_d\cos\beta\cos(\varphi(t))\dot{\varphi}(t)^2 - r_d\cos\beta\sin(\varphi(t))\ddot{\varphi}(t), \end{aligned} \tag{11}$$

$$\begin{aligned} a_{WC}(t) = \dot{W}_C(t) = {} & \tfrac{1}{2}(\ddot{w}_{v1}(l_{12},t) + \ddot{w}_{v2}(l_{22},t)) \\ & - r_d\cos\beta\sin(\varphi(t))\dot{\varphi}(t)^2 + r_d\cos\beta\cos(\varphi(t))\ddot{\varphi}(t). \end{aligned} \tag{12}$$

The geometric non-linear characteristics are considered for the tension-strain relation in the string by adopting the von Karman strain theory [20,21]. The tension-strain relation is expressed as

$$\varepsilon = EA(u' + \frac{1}{2}w'^2). \tag{13}$$

The dynamic tension in cables is expressed as spatially varying tension [22,23].

$$T_{vi}(x_v, t) = \overline{T}_{vi}(x_v, t) + EA(u'_{vi}(x_v, t) + \frac{1}{2}w'_{vi}(x_v, t)^2), \tag{14}$$

$$T_{ci}(x_c, t) = \overline{T}_{ci}(x_c, t) + EA(u'_{ci}(x_c, t) + \frac{1}{2}w'_{ci}(x_c, t)^2). \tag{15}$$

The weight component parallel to the catenary section is considered. The static tension $\overline{T}_{ci}(x_c, t)$, $\overline{T}_{vi}(x_v, t)$ in the inclined catenary section [24] and the vertical section of the ith cable can be represented as

$$\overline{T}_{ci}(x_c, t) = [M_i(t) + L_{vi}(t)\rho]g - (L_{ci} - x_c)\rho g \sin(\theta), \tag{16}$$

$$\overline{T}_{vi}(x_v, t) = M_i(t)g + (L_{vi}(t) - x_v)\rho g. \tag{17}$$

The equal load M_i of the ith cable, which depends on the angle φ of the conveyance, meets the following equation of static equilibrium

$$M_1 g + M_2 g = Mg, \tag{18}$$

$$M_1 g(S_1 + e\cos\varphi) = M_2 g(S_2 - e\cos\varphi), \tag{19}$$

where S_i is the distance between the ith cable and the center of the conveyance. And e is the eccentricity from the mass center of the conveyance, which always appears in the asymmetric loading. The virtual work is done by external forces can be expressed as

$$\begin{aligned}\delta W &= \delta W_{tc} + \delta W_{tv} + \delta W_{lc} + \delta W_{lv} + \delta W_s + \delta W_M + \delta W_{VM} + \delta W_{CM} + \delta W_{f_c} + \delta W_d \\ &= -\sum_{i=1}^{2}\int_{li0}^{li1-}(c_{tc}(\dot{w}_{ci} + V(t)w'_{ci})\delta w_{ci})dx_c - \sum_{i=1}^{2}\int_{li1+}^{li2}(c_{tv}(\dot{w}_{vi} + V(t)w'_{vi})\delta w_{vi})dx_v \\ &\quad - \sum_{i=1}^{2}\int_{li0}^{li1-}(c_{lc}(\dot{u}_{ci} + V(t)u'_{ci})\delta u_{ci})dx_c - \sum_{i=1}^{2}\int_{li1+}^{li2}(c_{lv}(\dot{u}_{vi} + V(t)u'_{vi})\delta u_{vi})dx_v \\ &\quad -c_s(V(t) + \dot{u}_{ci}(l_{i1-}, t))\delta u_{ci}(l_{i1-}, t) + Mg\delta cv + \sum_{i=1}^{2}\int_{li1+}^{li2}\rho g\delta u_{vi}(x, t)dx_v \\ &\quad + \sum_{i=1}^{2}\int_{li0}^{li1-}\rho g\cos(\theta)\delta w_{ci}(x, t)dx_c - (f_{cl}(t) + f_{cr}(t))\delta cw \\ &\quad -(f_{cl}(t) - f_{cr}(t))r_d\sin(\phi - \varphi(t))\delta\varphi(t) + \sum_{i=1}^{2}d_i(t)\delta u_{ci}(l_{i0}, t),\end{aligned} \tag{20}$$

where the virtual work δW_{tc}, δW_{tv}, δW_{lc}, δW_{lv} are done by transverse and longitudinal damping forces on catenary and vertical ropes respectively. δW_s is done by friction forces on head sheaves, δW_M, δW_{VM} are done by the gravity on the conveyance and the vertical ropes. δW_{CM} is done by the gravity component vertical to catenary ropes. δW_{f_c} is done by the counterforce $f_{cl}(t)$, $f_{cr}(t)$ from flexible guides, including forces and moments. δW_d is done by driving forces from drums. According to Eqs. (9) and (10), δcw, δcv which are transverse and longitudinal virtual displacements of the conveyance can be expressed by the virtual displacements of the ends of two cables.

$$\delta cv = \frac{1}{2}(\delta u_{v1}(l_{12}, t) + \delta u_{v2}(l_{22}, t)) - r_d cos\beta\sin(\varphi(t))\delta\varphi(t), \tag{21}$$

$$\delta cw = \frac{1}{2}(\delta w_{v1}(l_{12}, t) + \delta w_{v2}(l_{22}, t)) + r_d\cos\beta\cos(\varphi(t))\delta\varphi(t). \tag{22}$$

According to the Hamilton's principle [25,26],

$$\int_{t1}^{t2}(\delta E_k - \delta E_p + \delta W)dt = 0. \tag{23}$$

Using the Buckingham pi theorem [27,28], the dimensionless govern equation of cables can be obtained (i=1, 2, "^" means dimensionless variables).

$$(\hat{\ddot{u}}_{ci} + \hat{a}\hat{u}'_{ci} + 2\hat{V}\hat{\dot{u}}'_{ci} + \hat{V}^2\hat{u}''_{ci} + \hat{a}) + \hat{c}_v\hat{\dot{u}}_{ci} - \hat{E}\hat{A}(\hat{u}''_{ci} + \hat{w}'_{ci}\hat{w}''_{ci}) = -\hat{g}\cos(\theta), \tag{24}$$

$$\begin{aligned}&(\hat{\ddot{w}}_{ci} + \hat{a}\hat{w}'_{ci} + 2\hat{V}\hat{\dot{w}}'_{ci} + \hat{V}^2\hat{w}''_{ci}) + \hat{c}_w\hat{\dot{w}}_{ci} - (\hat{\overline{T}}_{ci}\hat{w}''_{ci} + \hat{\overline{T}}'_{ci}\hat{w}'_{ci} \\ &\quad + \hat{E}\hat{A}(\hat{u}''_{ci} + \hat{w}'_{ci}\hat{w}''_{ci})\hat{w}'_{ci} + \hat{E}\hat{A}(\hat{u}'_{ci} + \tfrac{1}{2}\hat{w}'^2_{ci})\hat{w}''_{ci}) = -\hat{g}\sin(\theta),\end{aligned} \tag{25}$$

$$(\hat{\ddot{u}}_{vi} + \hat{a}\hat{u}'_{vi} + 2\hat{V}\hat{\dot{u}}'_{vi} + \hat{V}^2\hat{u}''_{vi} + \hat{a}) + \hat{c}_v\hat{\dot{u}}_{vi} - \hat{E}\hat{A}(\hat{u}''_{vi} + \hat{w}'_{vi}\hat{w}''_{vi}) = \hat{g}, \tag{26}$$

$$\begin{aligned}&(\hat{\ddot{w}}_{vi} + \hat{a}\hat{w}''_{vi} + 2\hat{V}\hat{\dot{w}}'_{vi} + \hat{V}^2\hat{w}''_{vi}) + \hat{c}_w\hat{\dot{w}}_{vi} - (\hat{\overline{T}}_{vi}\hat{w}''_{vi} + \hat{\overline{T}}'_{vi}\hat{w}'_{vi} \\ &\quad + \hat{E}\hat{A}(\hat{u}''_{vi} + \hat{w}'_{vi}\hat{w}''_{vi})\hat{w}'_{vi} + \hat{E}\hat{A}(\hat{u}'_{vi} + \tfrac{1}{2}\hat{w}'^2_{vi})\hat{w}''_{vi}) = 0,\end{aligned} \tag{27}$$

with three constant quantity T_0, ρ, L_0. The typical dimensionless variables in Eqs. (24)–(27) are showed as follow

$$\hat{u} = \frac{u}{L_0},\ \hat{w} = \frac{w}{L_0},\ \ \hat{x} = \frac{x}{L_0},\ \ \hat{t} = \frac{t}{L_0}\sqrt{\frac{T_0}{\rho}},$$
$$\widehat{M} = \frac{M}{\rho L_0},\ \ \widehat{EA} = \frac{EA}{T_0},\ \ \ \widehat{V} = V\sqrt{\frac{\rho}{T_0}},\ \ \ \hat{a} = \frac{a\rho L_0}{T_0},\ \ \ \hat{g} = \frac{g\rho L_0}{T_0},$$
$$\hat{d}_i = \frac{d_i}{T_0},\ \ \hat{J}_c = \frac{J_c}{\rho {L_0}^3},\ \ \ \ \hat{L}_{vi} = \frac{L_{vi}}{L_0},\ \ \hat{c}_w = \frac{c_w L_0}{T_0\sqrt{\frac{\rho}{T_0}}}.$$

Eqs. (24)–(27) govern the transverse-longitudinal coupled elastic displacements of each cable. The coupled static tensions $\widehat{\overline{T}}_{vi}$, $\widehat{\overline{T}}_{ci}$ in Eqs. (24)–(27) exist in different cables. They can be obtained by solving Eqs. (16) and (17) with nondimensionalization. T_0 is the gravity force of the conveyance and L_0 is the initial length of the cable. For clearly presentation, we drop the "^" sign of all state variables u, w and x in the following equations.

The system boundary conditions at drums and head sheaves are obtained as Eq. (28),

$$\hat{d}_i(t) + \widehat{\overline{T}}_{ci}(l_{i0},\ \ t) + \widehat{EA}\,(u'_{ci}(l_{i0},\ t) + \frac{1}{2}w'_{ci}(l_{i0},\ t)^2) + \frac{\widehat{\tilde{J}}_d(t)}{\hat{R}_d{}^2}(\ddot{u}_{ci}(l_{i0},\ t) + \hat{V}\,(t)) = 0, \tag{28}$$

$\widehat{\tilde{J}}_d$ is the nondimensional time-varying equal inertia moment of the drums, considering the mass varying of the cables winding on drums in the process of hoisting. The time-varying equal inertia moment of the drums $\tilde{J}_d$ without nondimensionalization can be obtained by combining the second and third items in Eq. (1),

$$\tilde{J}_d(t) = J_d + (L_{vi}(0) - L_{vi}(t))\rho R_d^2. \tag{29}$$

For the more accurate modeling of the drums, R_d in Eq. (29) would be replaced by a slight varying radius which is relate to varying layers of cables winding on the drums. The system boundary conditions at head sheaves are obtained as

$$\begin{aligned}&\frac{\hat{J}_s}{\hat{R}_s{}^2}(\ddot{u}_{ci}(l_{i1-},\ t) + \hat{V}\,(t)) - \widehat{\overline{T}}_{ci}(l_{i1-},\ t) - \widehat{EA}\,(u'_{ci}(l_{i1-},\ t) + \tfrac{1}{2}w_{ci}{}'(l_{i1-},\ t)^2)\\ &+ \widehat{\overline{T}}_{vi}(l_{i1+},\ t) + \widehat{EA}\,(u'_{vi}(l_{i1+},\ t) + \tfrac{1}{2}w'_{vi}(l_{i1+},\ t)^2) - \hat{c}_s(\dot{u}_{ci}(l_{i1-},\ t) + \hat{V}\,(t)) = 0,\end{aligned} \tag{30}$$

According to Coulomb's Law [29], considering the friction between cables and head sheaves, the relationship between the longitudinal elastic displacements of the cable at the first contact point and the second contact point on the head sheave is given by,

$$u_{ci}(l_{i1-},\ t) = u_{vi}(l_{i1+},\ t)e^{c_s d_s}, \tag{31}$$

where d_s is the length of the sticking zone between the point l_{i1-} and the point l_{i1+} on the head sheaves. Eq. (28) represents the boundary conditions at drums and Eqs. (30) and (31) represent the boundary conditions at head sheaves. The system boundary conditions at the conveyance can be obtained as

$$-\sum_{i=1}^{2}(\widehat{\overline{T}}_{vi}(l_{i2},\ t) + \widehat{EA}\,(u'_{vi}(l_{i2},\ t) + \frac{1}{2}{w'_{vi}}^2(l_{i2},\ t))) + \widehat{M}\hat{a}_{vc}(t) + \widehat{M}\hat{g} = 0, \tag{32}$$

$$\begin{aligned}&\hat{J}_c\ddot{\varphi}(t) + (\hat{f}_{cl}(t) - \hat{f}_{cr}(t))\hat{r}_d\sin(\phi - \varphi(t)) - \widehat{M}\hat{g}\hat{r}_d\cos\beta\sin(\varphi(t))\\ &- \widehat{M}\hat{a}_{vc}(t)\hat{r}_d\cos\beta\sin(\varphi(t)) + \widehat{M}\hat{a}_{wc}(t)\hat{r}_d\cos\beta\cos(\varphi(t))\\ &- (\hat{f}_{cl}(t) + \hat{f}_{cr}(t))\hat{r}_d\cos\beta\cos(\varphi(t)) = 0,\end{aligned} \tag{33}$$

$$\begin{aligned}&-\textstyle\sum_{i=1}^{2}[\widehat{\overline{T}}_{vi}(l_{i2},\ t) + \widehat{EA}\,(u'_{vi}(l_{i2},\ t) + \tfrac{1}{2}w'_{vi}(l_{i2},\ t)^2)]w'_{vi}(l_{i2},\ t)\\ &+\widehat{M}\hat{a}_{wc}(t) - (\hat{f}_{cl}(t) + \hat{f}_{cr}(t)) = 0.\end{aligned} \tag{34}$$

According to Fig. 2, the geometrical relationship between the angle of the conveyance and transverse and longitudinal displacements of ends of cables is described as

$$\varphi(t) = \frac{\hat{L}_{v1}(t) - \hat{L}_{v2}(t) + \left(\int_0^{l_{12}} u_{v1}(x_v,\ t)dx_v - \int_0^{l_{22}} u_{v2}(x_v,\ t)dx_v\right)}{\hat{l}_d}, \tag{35}$$

$$|w_{v1}(l_{12},\ t) - w_{v2}(l_{22},\ t)| = \hat{l}_d - \hat{l}_d\cos(\varphi(t)), \tag{36}$$

Eqs. (32)–(36) describe the coupled boundary among cable ends and the conveyance.

Signed f_{cl}, f_{cr} are counter forces from the left and right flexible guides which are tensioned strings with two fixed ends. They can be equal to a resultant moment M_F and a resultant force f_c on the center of the conveyance mass. According to the dynamic model of the tensioned string, the dimensionless counterforce from flexible guides can be written as

$$\ddot{w}_{gl}(c(t),t) - (\hat{T}_g w''_{gl}(c(t),t) + \tfrac{1}{2}\hat{E}_g\hat{A}_g w'_{gl}(c(t),t)^2 w''_{gl}(c(t),t) + \hat{E}_g\hat{A}_g w'_{gl}(c(t),t)^2 w''_{gl}(c(t),t)) = \hat{f}_{cl}(c(t),t), \tag{37}$$

$$\ddot{w}_{gr}(c(t),t) - (\hat{T}_g w''_{gr}(c(t),t) + \tfrac{1}{2}\hat{E}_g\hat{A}_g w'^2_{gr}(c(t),t) w''_{gr}(c(t),t) + \hat{E}_g\hat{A}_g w'^2_{gr}(c(t),t) w''_{gr}(c(t),t)) = \hat{f}_{cr}(c(t),t). \tag{38}$$

The fixed ends can be represented as $w_{gr}(0,t)=0$, $w_{gr}(L_g,t)=0$, $w_{gl}(0,t)=0$, $w_{gl}(L_g,t)=0$, the typical dimensionless variables in Eqs. (37) and (38) as follow

$$\hat{T}_g = \frac{T_g}{T_0}, \quad \hat{E}_g\hat{A}_g = \frac{E_gA_g}{T_0}, \quad \hat{f}_{cl} = \frac{f_{cl}}{T_0}, \quad \hat{f}_{cr} = \frac{f_{cr}}{T_0},$$

where E_g, A_g are Young's modulus and cross-sectional area of the flexible guides. T_g is pretension of the flexible guide. ρ_g is the mass per unit length of flexible guide. $c(t)$ is the position of the conveyance centroid on the flexible guides. Compared with the height of the conveyance, the flexible guide is very long, so the up-corner and the down−corner of the conveyance can be regarded being at the same position $c(t)$ on the flexible guide. $w_{gl}(c(t),t)$ represents the transverse elastic displacement of left flexible guide at the point $c(t)$. Similarly, $w_{gr}(c(t),t)$ represent the transverse elastic displacement of the right flexible guide at the point $c(t)$, showed in Fig. 2.

$$w_{gl}(c(t),t) = \frac{1}{2}(w_{v1}(l_{12},t) + w_{v2}(l_{22},t)) - \hat{r}_z\cos(\phi - |\varphi(t)|) + \left(\frac{1}{2}\hat{l}_t + \hat{l}_l\right), \tag{39}$$

$$w_{gr}(c(t),t) = \frac{1}{2}(w_{v1}(l_{12},t) + w_{v2}(l_{22},t)) + \hat{r}_z\cos(\phi - |\varphi(t)|) - \left(\frac{1}{2}\hat{l}_t + \hat{l}_l\right). \tag{40}$$

3. Discrete mathematical model

3.1. Discrete model of the cables

The mathematical model of the multi-cable winding hoister with double drums is an infinite dimensional distributed-parameter system. There are not accurate analytic solutions. In this paper, the approximate solution of the govern equations of the multi-cable winding hoister with double drums can be obtained by using the Finite Difference Method [3,30–32]. Spatial variables of catenary ropes and temporal variables of the whole system are discretized as $X = 1, 2, \cdots n_c$ and $T = 1, 2, \cdots m$ respectively. n_c is the total number of spatial samples in the catenary rope and m is the total number of temporal samples for the whole system. The $n_c \times m$ matrices $U_{ci}(X, T+1)$, $W_{ci}(X, T+1)$ are defined to represent the dimensionless longitudinal and transverse elastic displacements of the catenary ropes. The differential of $u_{ci}(x_c, t)$ can be approximated by the difference expansions

$$\dot{u}_{ci}(x_c,t) = \frac{U_{ci}(X,T+1) - U_{ci}(X,T)}{\Delta k}, \tag{41}$$

$$\ddot{u}_{ci}(x_c,t) = \frac{U_{ci}(X,T+1) - 2U_{ci}(X,T) + U_{ci}(X,T-1)}{\Delta k^2}, \tag{42}$$

$$u'_{ci}(x_c,t) = \frac{U_{ci}(X+1,T) - U_{ci}(X,T)}{\Delta h}, \tag{43}$$

$$u''_{ci}(x_c,t) = \frac{U_{ci}(X+1,T) - 2U_{ci}(X,T) + U_{ci}(X-1,T)}{\Delta h^2}, \tag{44}$$

$$\dot{u}'_{ci}(x_c,t) = \frac{U_{ci}(X,T) - U_{ci}(X-1,T) - U_{ci}(X,T-1) + U_{ci}(X-1,T-1)}{\Delta h \Delta k}, \tag{45}$$

where Δh, Δk are dimensionless spatial and time intervals. The differential of $w_{ci}(x_c,t)$ are similar to the Eqs. (41)–(45).

The lengths of vertical rope $L_{vi}(t)$ are time-varying. By introducing a new independent variable $\zeta_i = \frac{x_v}{L_{vi}(t)}$, the time-varying spatial domain $x_{vi} \in [0, L_{vi}(t)]$ is converted to the fixed domain $\zeta_i \in [0, 1]$ [3,32]. The following relational expression can be obtained as

$$u_{vi}(x_v,t) = u_{vi}(\zeta_i L_{vi}(t),t) = z_i(\zeta_i,t), \tag{46}$$

$$w_{vi}(x_v,t) = w_{vi}(\zeta_i L_{vi}(t),t) = h_i(\zeta_i,t). \tag{47}$$

The derivatives of u_{vi} with respect to x_v and t are related to those of z_i with respect to ζ_i and t.

$$\dot{u}_{vi} = \frac{dz_i}{dt} - \frac{\hat{v}(t)\zeta_i}{\hat{L}_{vi}(t)}\frac{dz_i}{d\zeta_i}, \tag{48}$$

$$u'_{vi} = \frac{1}{\hat{L}_{vi}(t)} \frac{d\hat{z}_i}{d\zeta_i}, \tag{49}$$

$$u''_{vi} = \frac{1}{\hat{L}^2_{vi}(t)} \frac{dz_i^2}{d\zeta_i^2}, \tag{50}$$

$$\dot{u}'_{vi} = \frac{1}{\hat{L}_{vi}(t)} \frac{\partial z_i}{\partial \zeta_i \partial t} - \frac{\hat{v}(t)\zeta_i}{\hat{L}^2_{vi}(t)} \frac{dz_i^2}{d\zeta_i^2} - \frac{\hat{v}(t)}{\hat{L}^2_{vi}(t)} \frac{dz_i}{d\zeta_i}, \tag{51}$$

$$\ddot{u}_{vi} = \frac{dz_i^2}{dt^2} - \frac{2\hat{v}(t)\zeta_i}{\hat{L}_{vi}(t)} \frac{\partial z_i}{\partial \zeta_i \partial t} - \frac{\hat{v}^2(t)\zeta_i^2}{\hat{L}^2_{vi}(t)} \frac{dz_i^2}{d\zeta_i^2} - \frac{(\hat{L}_{vi}(t)\hat{a}(t) - 2\hat{a}^2(t))\zeta_i}{\hat{L}^2_{vi}(t)} \frac{dz_i}{d\zeta_i}, \tag{52}$$

The differential of $z_i(\zeta_i, t)$ with fixed domain can be approximated by the difference expansions

$$\dot{z}_i(\zeta_i, t) = \frac{Z_i(\eta_i^j, T+1) - Z_i(\eta_i^j, T)}{\Delta k}, \tag{53}$$

$$\ddot{z}_i(\zeta_i, t) = \frac{Z_i(\eta_i^j, T+1) - 2Z_i(\eta_i^j, T) + Z_i(\eta_i^j, T-1)}{\Delta k^2}, \tag{54}$$

$$z'_i(\zeta_i, t) = \frac{Z_i(\eta_i^{j+1}, T) - Z_i(\eta_i^j, T)}{\Delta \eta}, \tag{55}$$

$$z''_i(\zeta_i, t) = \frac{Z_i(\eta_i^{j+1}, T) - 2Z_i(\eta_i^j, T) + Z_i(\eta_i^{j-1}, T)}{\Delta \eta^2}, \tag{56}$$

$$\dot{z}'_i(\zeta_i, t) = \frac{Z_i(\eta_i^j, T) - Z_i(\eta_i^{j-1}, T) - Z_i(\eta_i^j, T-1) + Z_i(\eta_i^{j-1}, T-1)}{\Delta \eta \Delta k}, \tag{57}$$

where ζ_i is discretized as $0 = \eta_i^1, \cdots, \eta_i^j, \cdots, \eta_i^{n_v} = 1 \quad (j = 1, \cdots, n_v)$, n_v are the total number of spatial samples in the vertical rope. $\Delta\eta$ is constant dimensionless spatial interval.

$$\Delta\eta = \frac{1}{n_v}. \tag{58}$$

The $n_v \times m$ matrices $Z_i(\eta_i^j, T+1)$, $H_i(\eta_i^j, T+1)$ are defined to represent the dimensionless longitudinal and transverse elastic displacements of the vertical ropes.

The longitudinal and transverse elastic displacements of the catenary and vertical ropes at the initial moment (T=0) can be expressed as

$T = 0$:

$$U_{ci}(X, 1) = U_{c0i}(X) \qquad W_{ci}(X, 1) = W_{c0i}(X),$$

$$Z_i(\eta_i^j, 1) = U_{v0i}(j) \qquad H_i(\eta_i^j, 1) = W_{v0i}(j),$$

where $U_{c0i}(X)$,$W_{coi}(X)$ are initial longitudinal and transverse displacements of the catenary ropes. $U_{v0i}(j)$,$W_{voi}(j)$ are initial longitudinal and transverse displacements of vertical ropes.

$T = 1$:

By using the Taylor's series, the $U_{ci}(X, 2)$, $W_{ci}(X, 2)$, $Z_i(j, 2)$, $H_i(j, 2)$ can be obtained approximately based on $U_{ci}(X, 1)$, $W_{ci}(X, 1)$, $Z_i(j, 1)$, $H_i(j, 1)$.

$T \geq 2$:

Substituting the expressions (41–45) into the dynamic model (24) and (25), the discrete model of catenary ropes can be expressed as

$$\begin{aligned} &\Gamma(\chi_i) = 0 \\ &\Phi(\chi_i) = 0, \end{aligned} \tag{59}$$

where,

$$\begin{aligned} \chi_i = [&U_{ci}(X, T+1), U_{ci}(X-1, T+1), U_{ci}(X, T), U_{ci}(X+1, T), \\ &U_{ci}(X-1, T), U_{ci}(X, T-1), U_{ci}(X-1, T-1), W_{ci}(X, T+1), W_{ci}(X-1, T+1), \\ &W_{ci}(X, T), W_{ci}(X+1, T), W_{ci}(X-1, T), W_{ci}(X, T-1), W_{ci}(X-1, T-1)] \end{aligned} \tag{60}$$

The current longitudinal and transverse dimensionless elastic displacements $U_{ci}(X, T+1)$, $W_{ci}(X, T+1)$ of catenary ropes can be

obtained by solving the equation set (59). Substituting the expression Eqs. (48)–(57) into the Eqs. (26) and (27), the discrete model of vertical ropes can be expressed as

$$\begin{aligned} &\Theta(\varsigma_i) = 0 \\ &\Xi(\varsigma_i) = 0, \end{aligned} \tag{61}$$

where,

$$\begin{aligned} \varsigma_i = [&Z_i(\eta_i^j, T+1),\ Z_i(\eta_i^{j-1}, T+1),\ Z_i(\eta_i^j, T),\ Z_i(\eta_i^{j+1}, T), \\ &Z_i(\eta_i^{j-1}, T),\ Z_i(\eta_i^j, T-1),\ Z_i(\eta_i^{j-1}, T-1),\ H_i(\eta_i^j, T+1),\ H_i(\eta_i^{j-1}, T+1) \\ &H_i(\eta_i^j, T),\ H_i(\eta_i^{j+1}, T),\ H_i(\eta_i^{j-1}, T),\ H_i(\eta_i^j, T-1),\ H_i(\eta_i^{j-1}, T-1)], \end{aligned} \tag{62}$$

The fixed domain variables $Z_i(\eta_i^j, T+1)$, $H_i(\eta_i^j, T+1)$ can be obtained by solving the equation set (61). Casting $Z_i(\eta_i^j, T+1)$, $H_i(\eta_i^j, T+1)$ into the discrete expressions of Eqs. (46) and (47), the longitudinal and transverse elastic displacements $u_{vi}(x_v, t)$, $w_{vi}(x_v, t)$ at temporal point $t = T+1$ and spatial point $x_v = \hat{L}_{vi}(T+1)\eta_i^j$ can be obtained. The discrete processes of the boundary conditions are the same with the above process, which are not showed here for the sake of brevity.

3.2. Discrete model of the flexible guide

Spatial variables of the flexible guide are discretized as $X_g = 1, 2, \cdots n_g$. n_g is the total number of spatial samples in the flexible guide. The elastic displacements of left and right flexible guides can be discretized as

$$\begin{aligned} W_{gr}(X_g, T+1) = &\tfrac{1}{2}(U_{v1}(n_v, T+1) + U_{v2}(n_v, T+1)) \\ &+ \hat{r}_z \cos(\phi - |\varphi(T)|) - (\tfrac{1}{2}\hat{l}_t + \hat{l}_l), \end{aligned} \tag{63}$$

$$\begin{aligned} W_{gl}(X_g, T+1) = &\tfrac{1}{2}(U_{v1}(n_v, T+1) + U_{v1}(n_v, T+1)) \\ &- \hat{r}_z \cos(\phi - |\varphi(T)|) + (\tfrac{1}{2}\hat{l}_t + \hat{l}_l). \end{aligned} \tag{64}$$

The position point X_g represents the discrete positions of the conveyance on the flexible guides

$$X_g = \mathrm{INT}\left(\frac{c(t)}{\Delta h_g}\right) + 1, \tag{65}$$

where $\Delta h_g = L_g/(n_g - 1)$ is the spatial interval of the flexible guide. INT is the integer function to obtain the max integer less than independent variables. Other discrete position points of the flexible guide are approximately distributed on the line between $W_{gl}(X_g, T+1)$,$W_{gr}(X_g, T+1)$ and fixed ends of the flexible guide, showed in Fig. 2. The counterforce from flexible guides can be discretized as

$$\begin{aligned} \hat{F}_{gl}(X_g, T+1) = &\frac{W_{gl}(X_g, T+1) - 2W_{gl}(X_g, T) + W_{gl}(X_g, T-1)}{\Delta k^2} \\ &-\left(\hat{T}_g \frac{W_{gl}(X_g+1, T) - 2W_{gl}(X_g, T) + W_{gl}(X_g-1, T)}{\Delta h_g{}^2}\right. \\ &+\frac{3}{2}\hat{E}_g\hat{A}_g \frac{(W_{gl}(X_g, T) - W_{gl}(X_g-1, T))^2}{\Delta h_g{}^2} \\ &\left.\times\frac{W_{gl}(X_g+1, T) - 2W_{gl}(X_g, T) + W_{gl}(X_g-1, T)}{\Delta h_g{}^2}\right), \end{aligned} \tag{66}$$

$$\begin{aligned} \hat{F}_{gr}(X_g, T+1) = &\frac{W_{gr}(X_g, T+1) - 2W_{gr}(X_g, T) + W_{gr}(X_g, T-1)}{\Delta k^2} \\ &-\left(\hat{T}_g \frac{W_{gr}(X_g+1, T) - 2W_{gr}(X_g, T) + W_{gr}(X_g-1, T)}{\Delta h_g{}^2}\right. \\ &+\frac{3}{2}\hat{E}_g\hat{A}_g \frac{(W_{gr}(X_g, T) - W_{gr}(X_g-1, T))^2}{\Delta h_g{}^2} \\ &\left.\times\frac{W_{gr}(X_g+1, T) - 2W_{gr}(X_g, T) + W_{gr}(X_g-1, T)}{\Delta h_g{}^2}\right). \end{aligned} \tag{67}$$

4. Numerical simulation

The mathematical model is used to predict and analyze the dynamic behavior of a multi-cable double drum winding hoister under the ultra-deep, high-speed, heavy-load conditions. Typical parameters of the multi-cable winding double drum hoister for long distance transport used in simulation are showed in Tables 1 and 2.

The initial transverse displacements of cables are defined as zeros. The longitudinal elastic displacements of the catenary and

Table 1
Simulation parameters of the multi-cable double drum winding hoister.

Parameters of the hoister values	
Vertical length L_{vi} (t) (m)	2000
Catenary length L_{ci} (t) (m)	85
Cable effective steel area A (m^2)	3×10^{-3}
Cable effective Young's Modulus E(N/m^2)	1.53×10^{11}
Cable linear density ρ(kg/m)	8.02
Total hoisted mass M (kg)	10×10^{4}
Sheave wheel moment of inertia J_s (kg/m^2)	1.52×10^{4}
Winder drum moment of inertia J_d (kg/m^2)	3×10^{4}
Winder drum radius R_d (m)	2.5
Sheave wheel radius R_d (m)	2.5
Sticking zone on sheaves d_s (m)	2.8
Coil cross-over arcα(rad)	0.2
Damping coefficient c_v	0.5
Damping coefficient c_w	0.1
Damping coefficient c_s	0.5
Friction coefficient between head sheave and cables	0.01
Total hoisting time t (s)	133
Tension in the flexible guide T_g (N)	9×10^{6}
Effective steel area of the flexible guide A_g (m^2)	3×10^{-3}
Young's Modulus of the flexible guide E_g(N/m^2)	1.53×10^{11}
Length of the flexible guide L_g (m)	2000

Table 2
The dimensions of the conveyance. (showed in Fig. 2).

Conveyance dimension	r_d(m)	r_z(m)	l_d(m)	l_t(m)	l_l(m)	l_g(m)	l_z(m)	β(rad)	ϕ(rad)
values	3.53	3.90	5	5	0.5	5	6	0.785	0.696

vertical ropes are defined as Eqs. (68) and (69).

$$u_{ci}(x_c, 0) = \frac{M_i g + L_{vi}(0)\rho g}{EA} - \frac{(L_{ci} - x_c)\rho g \sin(\theta)}{EA}, \tag{68}$$

$$u_{vi}(x_v, 0) = \frac{M_i g + \rho g (L_{vi}(0) - x_v)}{EA}. \tag{69}$$

In this section, the dynamic behaviors of the hoister in the ascending cycle are showed, because vibration energy of cables would increase in the upward movement [33]. It would introduce non-stabilizing effect into system. The target position of the cage in upward movement is showed in the Fig. 3. The max hoisting velocities is 18 m/s in the simulation. Usually, the hoisting velocity more than 15 m/s can be defined as "high speed" for the deep mining hoister.

The conveyance eccentricity and drum radius inconformity are applied into the hoister as the unbalance factors. The vibration

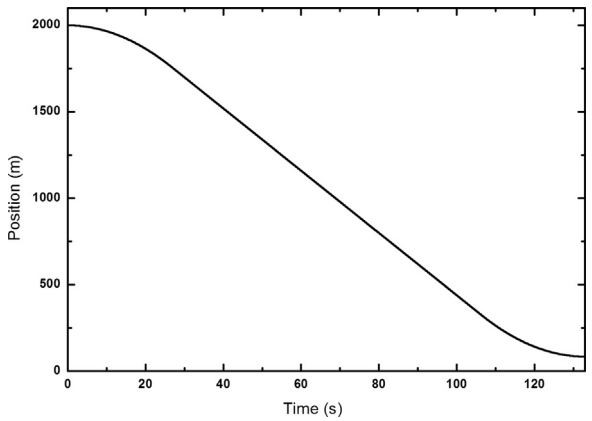

Fig. 3. The target movement curve of the hoister in the upward movement with the max velocity 18 m/s and the max acceleration 0.68 m/s^2.

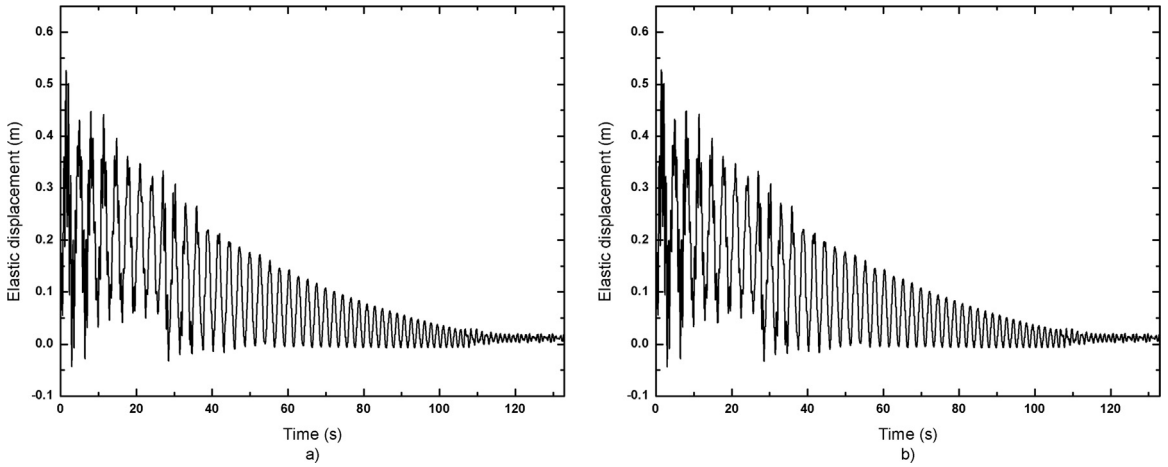

Fig. 4. In the case of 0.05 m conveyance eccentricity. a) The longitudinal elastic displacement at the midpoint ($L_{v1}(t)/2$) of the vertical rope 1. b) The longitudinal elastic displacement at the midpoint ($L_{v2}(t)/2$) of the vertical rope 2.

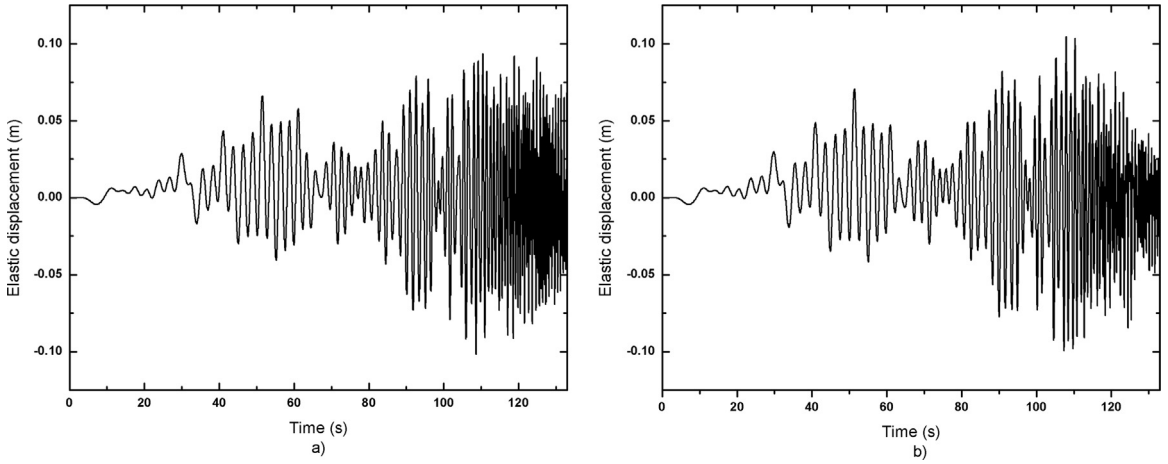

Fig. 5. In the case of 0.05 m conveyance eccentricity. a) The transverse elastic displacement at the midpoint ($L_{v1}(t)/2$) of the vertical rope 1. b) The transverse elastic displacement at the midpoint ($L_{v2}(t)/2$) of the vertical rope 2.

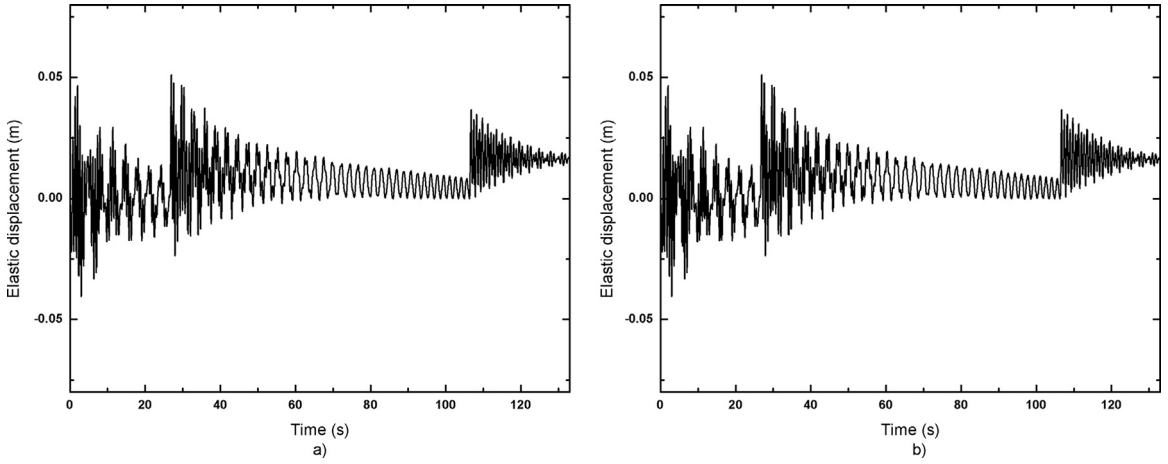

Fig. 6. In the case of 0.05 m conveyance eccentricity. a) The longitudinal elastic displacement at the midpoint of the catenary rope 1. b) The longitudinal elastic displacement at the midpoint of the catenary rope 2.

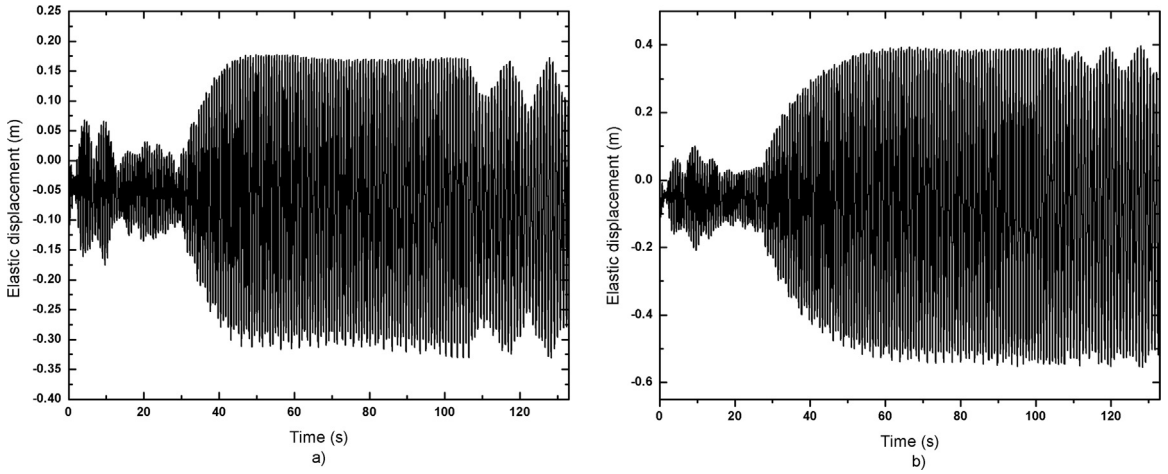

Fig. 7. In the case of 0.05 m conveyance eccentricity. a) The transverse elastic displacement at the midpoint of the catenary rope 1. b) The transverse elastic displacement at the midpoint of the catenary rope 2.

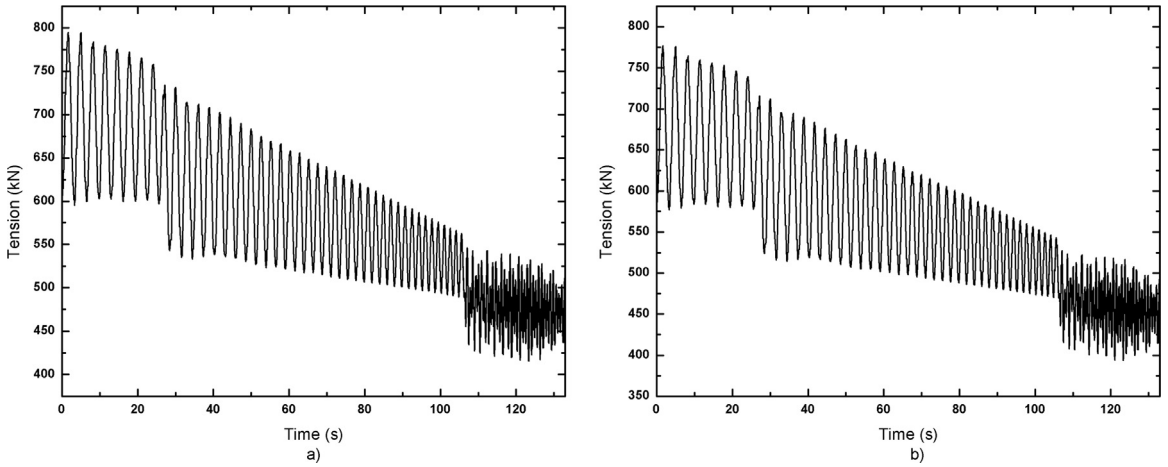

Fig. 8. In the case of 0.05 m conveyance eccentricity. a) Dynamic tension at the midpoint $(L_{v1}(t)/2)$ of the vertical rope 1. b) Dynamic tension at the midpoint $(L_{v2}(t)/2)$ of the vertical rope 2.

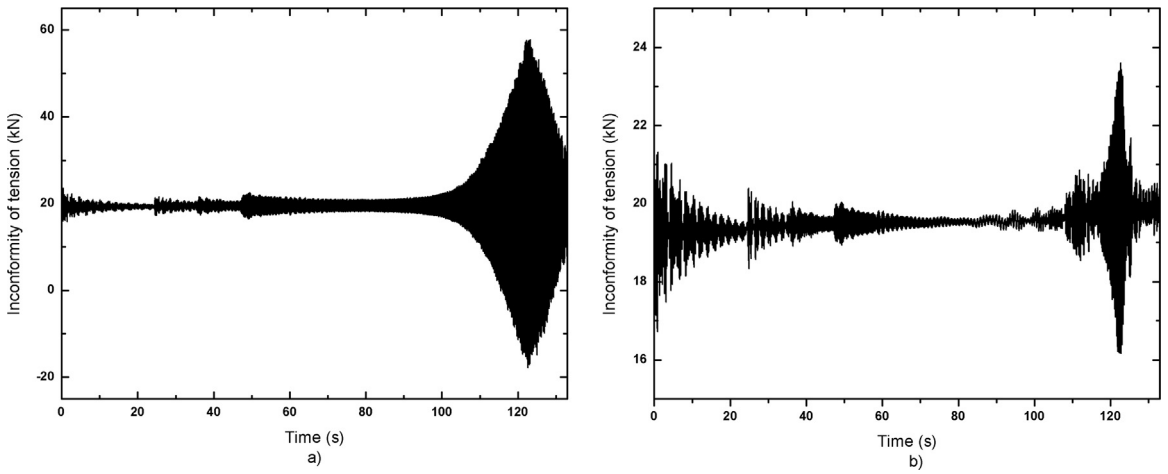

Fig. 9. In the case of 0.05 m conveyance eccentricity. a) Inconformity of dynamic tension at midpoints $(L_{vi}(t)/2)$ of vertical ropes. b) Inconformity of dynamic tension at midpoints of catenary ropes.

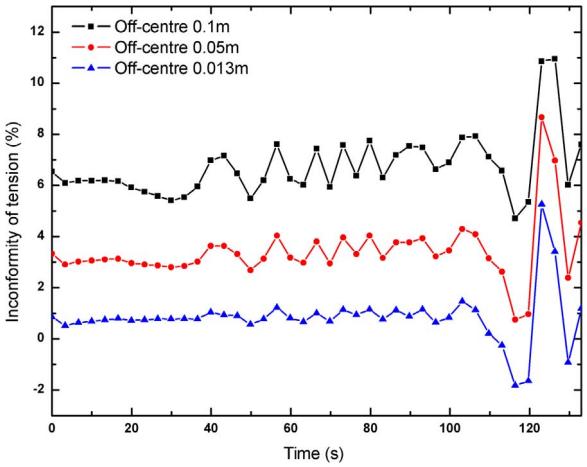

Fig. 10. The inconformity rate of dynamic tension at midpoints $(L_{vi}(t)/2)$ of vertical ropes with different conveyance eccentricities.

response and dynamic tension in cables would be observed.

4.1. Conveyance eccentricity

In the practical mine engineering, the conveyance eccentricity appears frequently in the process of loading. It is an important factor to the instabilities of the hoister system, especially for the multi-cable winding hoisters used in long distance transport. The dynamic responses of the hoister with 0.05 m conveyance eccentricity are presented in Figs. 4–9. The inconformity rates of dynamic tension under different conveyance eccentricity are showed in Fig. 10.

It can be observed from Figs. 4–7 that the maximum displacement of the longitudinal vibration at the midpoint $(L_{vi}(t)/2)$ of the vertical ropes are larger than that of transverse vibration due to the large cable tension introduced by heavy load. Adversely, the longitudinal elastic displacements at the midpoint of the catenary ropes are smaller than corresponding transverse elastic displacements. Because one gravity component of the self-weight of catenary ropes reduce the cable tension caused by heavy load. The other gravity component of the catenary rope arouses transverse elastic displacements of the catenary ropes. It is noteworthy that the amplitude and frequency of transverse vibration at midpoint of vertical ropes increase during the upward movement, because the vibration energy would increase with the fast decrease of the length of the cable [32].

According to Fig. 8, the dynamic tension in cable 1 is larger than that in cable 2 slightly, due to the bias of the conveyance centroid towards to cable 1.

It is showed in Fig. 9 that no matter in vertical or catenary ropes, the inconformity of dynamic tension would increase in the later of upward movement. The reason is that the vibration energy of cables would increase in the later of the upward movement [32], especially for the transverse vibration of the cables.

A principle can be obtained from Fig. 10 is that the inconformity of dynamic tension would be positively related to the amplitude of the conveyance eccentricity. In the practical engineering, the conveyance eccentricity of the similar size hoister should be limited

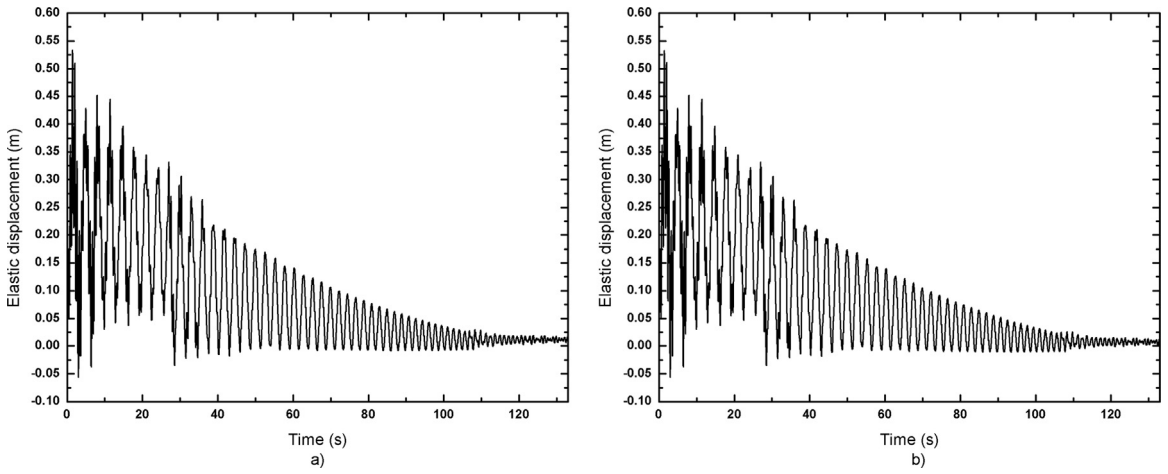

Fig. 11. In the case of 0.05 mm drum radius inconformity. a) The longitudinal elastic displacement at the midpoint $(L_{v1}(t)/2)$ of the vertical rope 1. b) The longitudinal elastic displacement at the midpoint $(L_{v2}(t)/2)$ of the vertical rope 2.

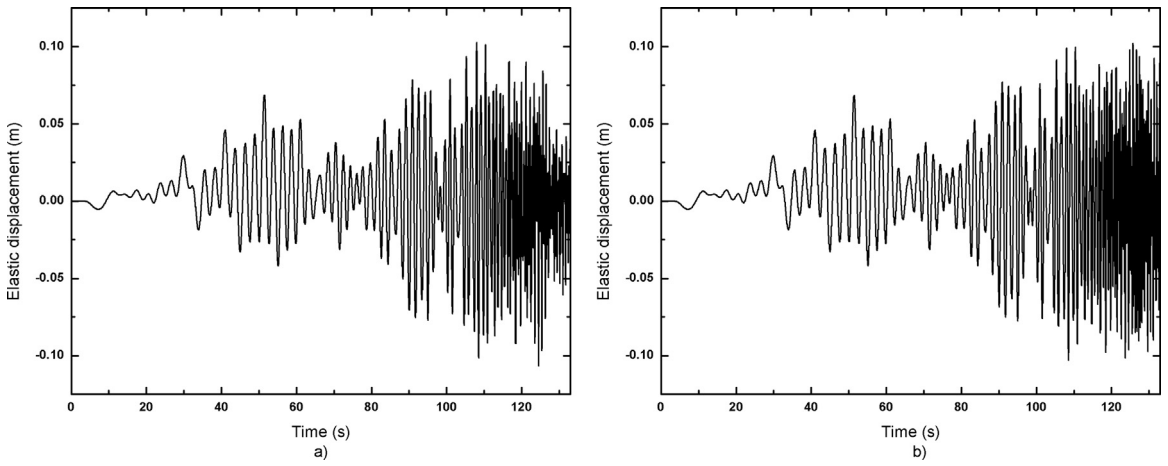

Fig. 12. In the case of 0.05 mm drum radius inconformity. a) The transverse elastic displacement at the midpoint ($L_{v1}(t)/2$) of the vertical rope 1. b) The transverse elastic displacement at the midpoint ($L_{v2}(t)/2$) of the vertical rope 2.

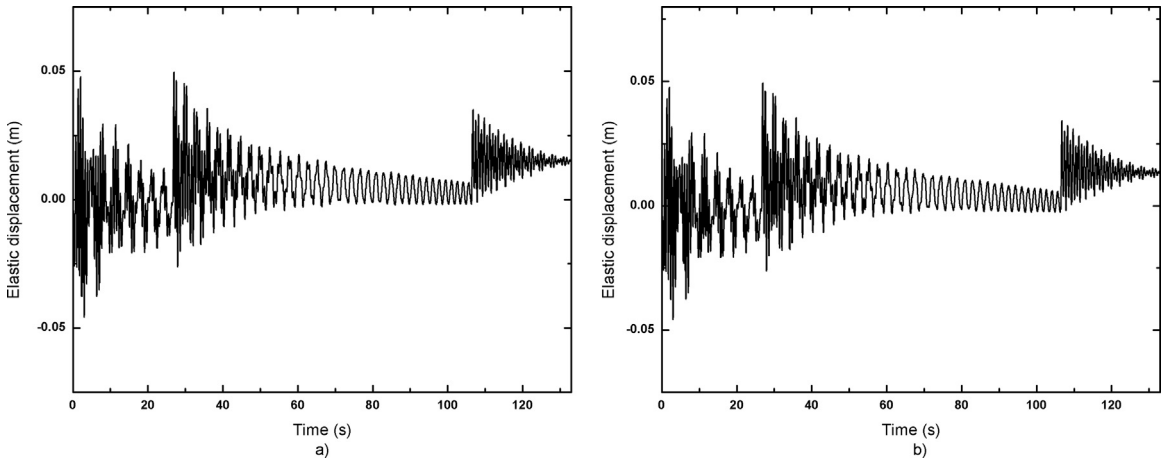

Fig. 13. In the case of 0.05 mm drum radius inconformity. a) The longitudinal elastic displacement at the midpoint of the catenary rope 1. b) The longitudinal elastic displacement at the midpoint of the catenary rope 2.

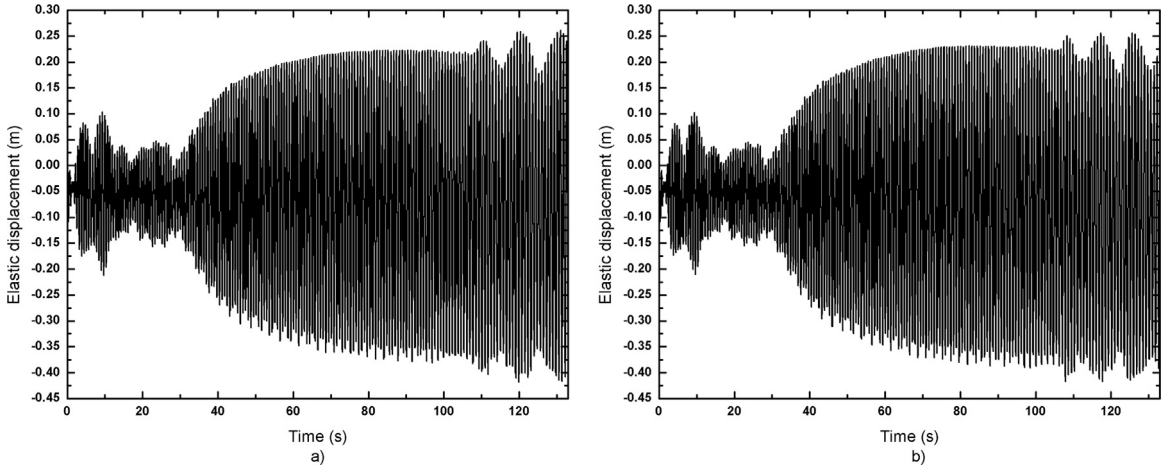

Fig. 14. In the case of 0.05 mm drum radius inconformity. a) The transverse elastic displacement at the midpoint of the catenary rope 1. b) The transverse elastic displacement at the midpoint of the catenary rope 2.

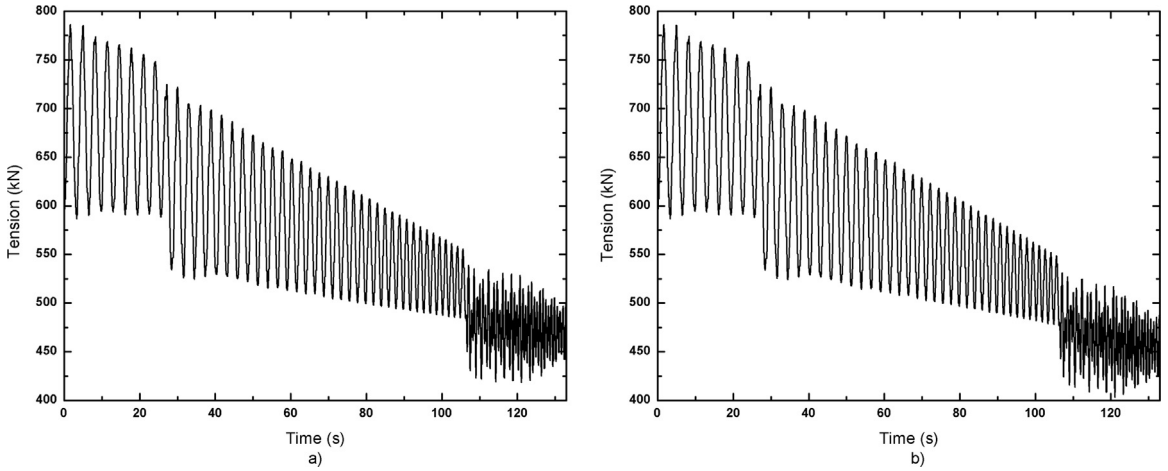

Fig. 15. In the case of 0.05 mm drum radius inconformity. a) Dynamic tension at the midpoint $(L_{v1}(t)/2)$ of the vertical rope 1. b) Dynamic tension at the midpoint $(L_{v2}(t)/2)$ of the vertical rope 2.

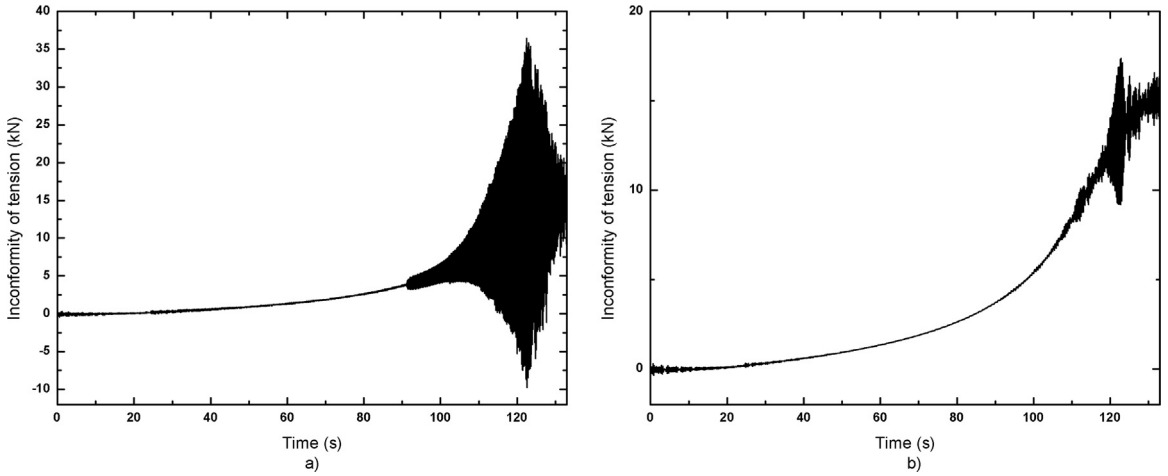

Fig. 16. In the case of 0.05 mm drum radius inconformity. a) Inconformity of dynamic tension at midpoints $(L_{vi}(t)/2)$ of vertical ropes. b) Inconformity of dynamic tension at midpoints of catenary ropes.

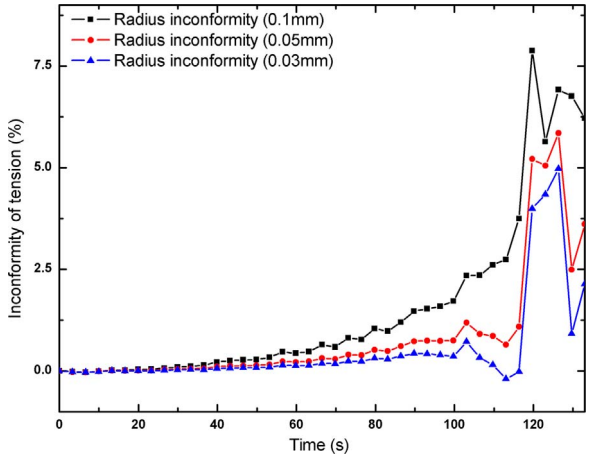

Fig. 17. Inconformity rates of dynamic tension at midpoints of vertical ropes with different radius inconformity between two drums.

in less 0.013 m to guarantee the dynamic tension inconformity in the acceptable range (5%) of the mining industry.

4.2. Radius inconformity between driving drums

Inconformity radius of driving drums is a common phenomenon in winding hoisters due to the errors of mechanical process. It would result to the enlargement of tension inconformity between cables. The dynamic responses of the hoister under 0.05mm drum radius inconformity are showed in Figs. 11–16. The inconformity rates of dynamic tension with different inconformity of drum radius are showed in Fig. 17.

According to Fig. 15, the dynamic tension in cable 1 is slightly larger than that in cable 2, which appears more obviously in the final stage due to the accumulated error of the radius inconformity between two driving drums.

According to Fig. 16, the inconformity of dynamic tensions increases gradually in the upward movement because of the accumulated movement inconformity which is caused by the radius inconformity between two drums. There is the substantial increase in dynamic tension inconformity during the latter of the upward movement due to intensified vibration, which is similar to the case of the conveyance eccentricity.

From Fig. 17, it can be observed that the inconformity of dynamic tension would be positively related to the inconformity between the two drum radiuses. In the practical engineering, the mechanical process error of drum radius of the similar size hoister should be limited in 0.03mm to guarantee the dynamic tension inconformity in the acceptable range (5%) of the mining industry.

5. Conclusions

In this paper, the model of a multi-cable winding hoister with double drums has been built via Hamilton principle, which is a strong coupled, time varying, nonlinear distributed-parameter system. Each cable which consists of the catenary and vertical ropes is modeled as the axially moving string with the coupled transverse-longitudinal nonlinear vibration. The catenary and vertical ropes are represented as the constant-length inclined string and the varying-length vertical string respectively and they are coupled at the head sheave. The friction between the cable and the sheave is also considered at the head sheave. Coupling between different cables are described through the dynamic and kinematic equations of the conveyance. The time-varying equal inertia moment of winding drums is obtained by considering varying mass of the cables winding on the drums. In addition, the dynamic model of the flexible guide which was always approximated as a spring-damping system is built as a tensioned string with two fixed ends in this paper. The dynamic characteristics of interaction between the flexible guides and the conveyance are considered in the modeling through calculating the lateral displacement of the conveyance corner and the reactions forces from flexible guides. The Finite Difference Method is adopted to discretize this infinite dimensional distributed-parameter model and the approximate solution is obtained. The conveyance eccentricity and drum radius inconformity are applied into the model of the hoister as the unbalance factors in simulation. The coupled transverse-longitudinal vibration and the dynamic tension of cables in the multi-cable winding hoister are analyzed under the long-distance, high-speed, heave-load condition. Some dynamic behavior of vibration and tension in cables are observed. The maximum amplitude of the longitudinal vibration is larger than that of the transverse vibration at the midpoint of the vertical rope. Adversely, the maximum amplitude of longitudinal vibration is smaller than that of transverse vibration at the midpoint of the catenary rope. In the case of the drum radius inconformity, the inconformity of dynamic tension increases gradually in the upward movement. In both cases of the conveyance eccentricity and the drum radius inconformity, the inconformity of dynamic tension between cables will rise substantially in later of the upward movement. Some principles on the inconformity of dynamic tension between different cables have been proposed. For a similar size multi-cable winding hoister in the mining engineering, the conveyance eccentricity and the drum radius inconformity should be restricted in less 0.013 m and 0.03 mm respectively to guarantee the dynamic tension inconformity in the acceptable range (5%) of the mining industry.

Acknowledgment

The authors gratefully acknowledge the fund support from the National Basic Research Program of China [2014CB049404].

References

[1] A. Carbogno, Mine hoisting in deep shafts in the 1st half of 21st Century, Acta Montan. Slov. 7 (2002) 188–192.
[2] W.D. Zhu, N.A. Zheng, Exact response of a translating string with arbitrarily varying length under general excitation, J. Appl. Mech. 75 (2008) 0310031–03100314.
[3] W.D.Zhu, Y.Chen, Forced response of translating media with variable length and tension: application to high-speed elevators. Proceedings of the Institution of Mechanical Engineers, Part K: Journal of Multi-body Dynamics. 219,35–53, 2005.
[4] W. He, S.S. Ge, D.Q. Huang, Modeling and vibration control for a nonlinear moving string with output constraint, IEEE/ASME Trans. Mechatron. 20 (2015) 1886–1897.
[5] S.H. Sandilo, W.T. van Horssen, On variable length induced vibrations of a vertical string, J. Sound Vib. 333 (2014) 2432–2449.
[6] S.H. Sandilo, W.T. van Horssen, On a cascade of autoresonances in an elevator cable system, Nonlinear Dyn. 80 (2015) 1613–1630.
[7] K.Wu, W.D.Zhu, Parametric instability in a stationary string sith a periodically varying length. in: Proceedings of the 26th Conference on Mechanical Vibration and Noise Buffalo, New York, USApp. 17–20, 2014.
[8] P. Zhang, C.M. Zhu, L.J. Zhang, Analysis of forced coupled longitudinal-transverse vibration of flexible hoisting systems with varying length, Eng. Mech. 25 (2008) 202–207.
[9] A. Kumaniecka, J. Niziol, Dynamic stability of a rope with slow variability of the parameters, J. Sound Vib. 178 (1994) 211–226.
[10] S. Kaczmarczyk, W. Ostachowicz, Transient vibration phenomena in deep mine hoisting cables, Part 1: Mathematical model, J. Sound Vib. 262 (2003) 219–244.
[11] S. Kaczmarczyk, W. Ostachowicz, Transient vibration phenomena in deep mine hoisting cables, Part 2: numerical simulation of the dynamic response, J. Sound

Vib. 262 (2003) 245–289.
[12] N.G. Garkusha, V.I. Dvornikov, Equations of motion for a mine elevator as a one-dimensional elastic structure, Prikl. Mekhanika 5 (1969) 125–128.
[13] Y. Terumichi, M. Ohtsuka, M. Yoshizawa, Nonstationary vibrations of a string with time-varying length and a mass-spring system attached at the lower end, Nonlinear Dyn. 12 (1997) 39–55.
[14] W.D. Zhu, G.Y. Xu, Vibration of elevator cables with small bending stiffness, J. Sound Vib. 263 (2003) 679–699.
[15] M.H. Ghayesh, M. Amabili, M.P. Païdoussis, Nonlinear vibrations and stability of an axially moving beam with an intermediate spring support: two-dimensional analysis, Nonlinear Dyn. 70 (2012) 335–354.
[16] M.H. Ghayesh, Stability characteristics of an axially accelerating string supported by an elastic foundation, Mech. Mach. Theory 44 (2009) 1964–1979.
[17] Y.V. Chirkov, Taking account of the hysteresis guide devices in problems of the of a shaft elevator, Prikl. Mekhanika 9 (1973) 122–125.
[18] K. Wang, B.Y. Wang, C.C. Yang, Research on the multi-step straightening for the elevator guide rail, Procedia Eng. 16 (2011) 459–466.
[19] C.Dimitriou, A.Whillier, Vibrations in winding ropes: an appraisal. in: proceedings of the SAIMechE Hoisting Conference, Johannesburg, South Africapp. 1–13, 1973.
[20] M.A. Crisfield, Non-Linear Finite Element Analysis of Solids and Structures, John Wiley and Sons, Chichester, 1991.
[21] J. Chung, A.S. Han, Vibration of an axially moving string with geometric non-linearity and translating acceleration, J. Sound Vib. 240 (2001) 733–746.
[22] Q.C. Nguyen, K.S. Hong, Simultaneous control of longitudinal and transverse vibrations of an axially moving string with velocity tracking, J. Sound Vib. 331 (2012) 3006–3019.
[23] T.C. Li, Z.C. Hou, J.F. Li, Stabilization analysis of a generalized nonlinear axially moving string by boundary velocity feedback, Automatica 44 (2008) 498–503.
[24] X.D. Zhou, S.Z. Yan, F.L. Chu, In-plane free vibrations of an inclined taut cable, J. Vib. Acoust. Trans. ASME 133 (2011) 0310011–0310019.
[25] D.B. McIver, Hamilton's principle for systems of changing mass, J. Eng. Math. 7 (1973) 249–261.
[26] U. Lee, I. Jang, On the boundary conditions for axially moving beams, J. Sound Vib. 306 (2007) 675–690.
[27] W.D. Zhu, L.J. Teppo, Design and analysis of a scaled model of a high-rise, high-speed elevator, J. Sound Vib. 264 (2003) 707–731.
[28] S.M. Sahebkar, M.R. Ghavazi, S.E. Khadem, M.H. Ghayash, Nonlinear vibration analysis of an axially moving drillstring system with time dependent axial load and axial velocity in inclined well, Mech. Mach. Theory 46 (2001) 743–760.
[29] D. Knittel, E. Laroche, D. Gigan, H. Koc, Tension control for winding systems with two-degrees-of-freedom h controllers, IEEE Trans. Ind. Appl. 39 (2003) 113–120.
[30] H. Ding, G.C. Zhang, L.Q. Chen, Supercritical vibration of nonlinear coupled moving beams based on discrete Fourier transform, Int. J. Non-Linear Mech. 47 (2012) 1095–1104.
[31] L.Q. Chen, W.J. Zhao, A numerical method for simulating transverse vibrations of an axially moving string, Appl. Math. Comput. 160 (2005) 411–422.
[32] W. Wang, J. Qiang, Finite difference method for simulating transverse forced-vibration of elevator suspended system, J. Vib. Eng. 27 (2014) 180–185.
[33] W.D. Zhu, J. Ni, Energetics and stability of translating media with an arbitrarily varying length, J. Vib. Acoust. Trans. ASME 122 (2000) 295–304.